Performance Analysis of Alexnet for Classification of Knee Osteoarthritis

T.Sivakumari[a], R.Vani[b,*]

[a] Research Scholar, Department of Electronics and Communication, SRM Institute of Science and Technology, Ramapuram, Chennai, India
[b] Professor, Department of Electronics and Communication, SRM Institute of Science and Technology, Ramapuram, Chennai, India
[*]Corresponding author: vanir@srmist.edu.in

***Abstract*— In recent years, automated grading of knee osteoarthritis (KOA) has mostly been helpful in determining the extent to which the illness has progressed. Clinical examinations as well as a review of the radiographic images are now required to identify this condition. The progression of this condition may be slowed down by obtaining an accurate diagnosis and receiving medical care. X-rays and MRI images of the knee are the most important diagnostic tools for osteoarthritis. The KOA is diagnosed based on the radiologist's and clinician's experience over the years. Due to its recent fast development, deep learning technology, often known as artificial intelligence (AI), has become an often-used solution to medical concerns. This document outlines all of the several methods that have been presented by various researchers about the automated grading of KOA and also explains the performance of the AlexNet model for the purpose of classifying the severity of KOA. This will be done by comparing the model's performance to that of other models and assessing the results.**

***Keywords*— AlexNet, Automatic grading, Convolution Neural Network, Classification, Knee Osteoarthritis, Segmentation.**

DOI Number: 10.48047/nq.2022.20.19.NQ99151 **NeuroQuantology2022;20(19): 1686-1692**

I. INTRODUCTION

The inflammatory disorder known as arthritis may damage any number of joints in the body. There are over a hundred different types of arthritis, which may be categorized according to their symptoms. The two types of arthritis that are seen most often are osteoarthritis (OA) and rheumatoid arthritis (RA).

Osteoarthritis, also known as Wear and Tear arthritis or Degenerative Joint Disease, is the ailment that affects the musculoskeletal system more often than any other. People of advanced age are most often affected by this condition. This disease can be identified by the most prominent clinical features such as joint space narrowing (also known as JSN), the development of osteophytes, and sclerosis. There is a tissue that is called cartilage is responsible for connecting the bones which also cushions the ends of the bones so that there is no friction at the joint. When the cartilage is diseased or injured, the bones might rub against one other, which can lead to discomfort, swelling, and stiffness. In knees affected by knee osteoarthritis (KOA), there is a narrowing of the space between the bones, which is referred to as Joint Space Narrowing (JSN). The most common risk factors associated with osteoarthritis are being overweight or obese, having a low bone density, experiencing trauma, not getting enough exercise, and having a genetic predisposition. Due to the fact that joint replacement surgery can only be performed on patients in the early stages of osteoarthritis (OA), early diagnosis is the only option for reducing the burden of the disease and maintaining a healthy lifestyle. The results of the research indicate that there were 303 million cases of osteoarthritis of the hip and knee around the world in the year 2017. This article's goal is to provide a concise summary of the research that has been conducted by a number of different

researchers on the diagnosis and categorization of KOA and the severity of the condition by making use of straightforward radiography and also gives the performance analysis of AlexNet on classification of KOA.

Medical imaging techniques such as magnetic resonance imaging (MRI), computed tomography (CT), ultrasound, and plain radiography (X-rays) are used in order to identify the first symptoms of osteoarthritis (OA). X-rays are the most cost-effective method, in addition to being easily accessible and posing a lower risk than the other approaches. Kellgren-Lawrence (KL) grades are often used by clinicians in order to rate the severity of osteoarthritis (OA) by analyzing the plain radiographic images of knees with and without OA. The images of normal and damaged knee cartilage are shown in the above fig. 1.

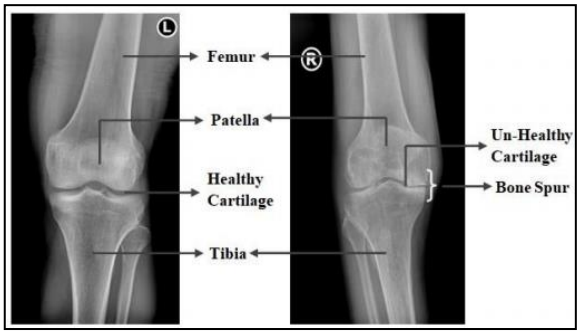

Fig. 1 Healthy and KOA affected Knee

A. *The KL Grading scale*

The KL grades are recognized all over the world as the standard for determining the severity of knee osteoarthritis. This grading system consists of five phases, numbered 0 through 4, as seen in fig. 2. Grade 0 indicates that the knees are in good health, while the succeeding grades (1-4) indicate that the severity of OA is growing.

B. *OARSI Grading System*

In the year 2006, the Osteoarthritis Research Society International (OARSI) was the organization that pioneered the introduction of an osteoarthritis cartilage histopathology evaluation system, also known as an OARSI system. This system had a grading component as well as a staging component. This approach may be broken down into two distinct phases: grading and staging. The ability of the system to differentiate between early and moderate OA is the system's defining characteristic. Tables 1 and 2 include a listing of the OARSI grades and stages.

TABLE 1
OSTEOARTHRITIS CARTILAGE HISTOPATHOLOGY ASSESSMENT SYSTEM

Grade	Explanation
Grade-0	surface intact, cartilage intact
Grade-1	Uneven but intact Possible features
Grade-2	surface discontinuity
Grade-3	vertical fissures
Grade-4	Erosion
Grade-5	Denudation

TABLE 2
STAGE ASSESSMENT OA CARTILAGE HISTOPATHOLOGY

Stage	%Involvement (Surface)
Stage-0	No OA activity seen
Stage-1	Less than 10%
Stage-2	Between 10 to 25%
Stage-3	Between 25 to 50%
Stage-4	> 50%

The following sections are included in the structure of the paper: section 2, related works, which provides a detailed description of the existing methodology; section 3, which provides details about datasets that are publicly available for KOA; section 4 describes the AlexNet architecture that was used in this work; section 5 discusses the results of AlexNet and compares them to the results of the existing method; and section 6 includes a conclusion and a discussion of the findings.

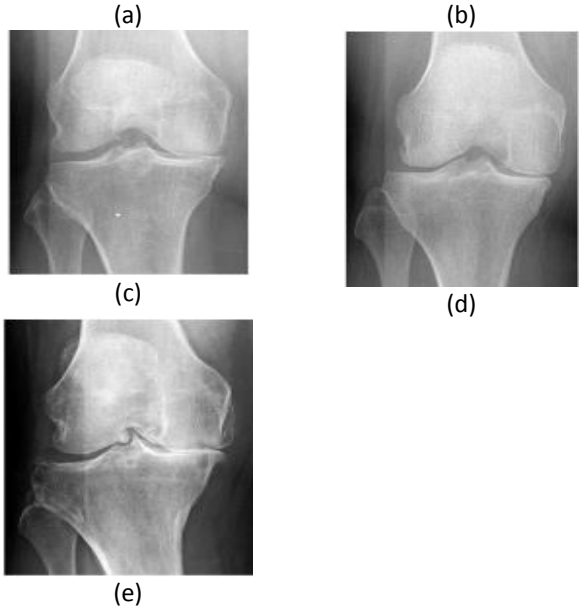

Fig. 2 Sample images of knees affected by osteoarthritis

The above images are graded according to the KL grading Scale. (a) A knee with no features of OA and is considered as Healthy Knee (KL-0). (b) An image of Doubtful OA Knee. There is a presence of unclear osteophytes and doubtful JSN (KL-1). (c) Sample image of Mild (Early) OA which has the definite osteophytes, Possible JSN (KL-2). (d) Moderate OA image having the symptoms of multiple osteophytes, definite JSN, sclerosis (KL-3). (e) This knee represents the severe OA because there are large osteophytes, Loss of JS, bone deformity (KL-4).

II. RELATED WORKS

It is standard practice for orthopedic doctors to recommend imaging tests like MRI and X-ray whenever a patient presents themselves. Segmentation is a procedure that may be used to automatically extract the additional information included in a picture. This is a necessary procedure for any kind of picture analysis. The results of a manual assessment may not be reliable until much later, and they are likely to include some inaccuracy. Segmenting a digital picture into its constituent parts often yields useful information for further processing. For the purpose of evaluating patient medical data, such as MRI (Magnetic Resonance Imaging), X-rays, CT (Computerized Tomography) scans, ECG (Electro Cardio Gram), and is recorded in DICOM format [1, 2].

Traditional segmentation techniques fall into three categories. Manual segmentation, in which seeds are placed over specified anatomic areas, is the first option and is used to accurately identify the borders of injured cartilage [3]. However, therapies are notoriously lengthy [4]. The doctor's skill and familiarity with human anatomy are crucial. The cartilage may also be automatically segmented using the second approach, known as automated segmentation. Active shape model, watershed, and k-nearest neighbor

categorization are a few examples [3]. For example, automated segmentation techniques like graph cuts and random walks may be combined with characteristics from human segmentation techniques in an interactive segmentation approach. In order to identify early stages of knee osteoarthritis, a variety of segmentation algorithms have been examined [5]. Sobel edge detection, which draws attention to the area of high spatial frequency, is a straightforward and reliable technique.

Numerous algorithms exist for grayscale image separation. However, the threshold segmentation technique is popular due to its effectiveness and ease of use [6]. The obvious joint gap was obtained by using an OTSU threshold segmentation approach to the ROI of the knee's joint space region; however the computation time is significant as the number of thresholds grows [7]. Table.3 provides a comprehensive analysis of the several segmentation methods that have been put into practice.

TABLE 3
ASSESSMENT OF SEGMENTATION METHODS IN KOA: A SURVEY AND COMPARISON

Ref. No.	Dataset & Data Type	No. of Images Used	Algorithm	Result
[8]	Own dataset & X-ray	5300	Dilated-Resnet, The Taguchi method is used to get the best results from deep learning.	Dice coefficients Femur-0.964, Tibia-0.942
[9]	OAI& MRI	76 subjects	Multi-atlas based segmentation technique, HOG feature descriptors	DSC- 88.22%, 85.84% for Femoral and Tibia respectively.
[10]	Own dataset & X-ray	532 X-ray Images	Otsu's segmentation, KNN, Texture based segmentation	Obtained accuracy for texture method-94.92%, Sobel method-91.16%, Otsu's method-96.80%, Prewitt method-97.55%
[11]	Own, OAI & X-ray	OAI-748 Own-370	Hourglass Network	Precision 93.48±0.44
[12]	OAI & X-ray	10	Flexible seeds labelling method	Observer 1: Dice coefficient-0.80±0.060, sensitivity 0.86±0.044 and specificity 0.99±0.001. Observer 2: Dice coefficient- 0.82 ± 0.043, sensitivity 0.85 ± 0.049 specificity 0.99 ± 0.001.
[13]	OAI & X-ray	4130	Single short Detector	94% of images having J >0.75

There are two methods available for studying knee osteoarthritis. The images are automatically categorized into KOA and non-KOA categories. Severity categorization of KOA by assessing pathogenic characteristics is another. Osteophytes, JSN, and subchondral sclerosis are the three most prevalent pathological characteristics in Knee OA [13]. These pathological characteristics are crucial in determining the grade of KOA using systems such as the KL and OARSI classifications. Some studies have employed composite grading systems, while others have quantified the severity of KOA based on a number of different pathological characteristics.

The factors of texture characteristics, Haralick, the First Four Movements, the statistical feature set, and the qualities of regions have all been taken into account [14]. The Random Forest Classifier was used to classify these characteristics. While the miss classified rate is somewhat higher in this study for each individual feature set, the suggested approach yields a more favorable outcome when applied to all of the available feature sets at once. However Joint space width analysis is one method used to diagnose knee osteoarthritis [15]. Clustering, Feature Selection, and Decision Making are all employed in the suggested technique [16] to anticipate the development of JSN using the interdisciplinary data from OAI. LR model included data from both legs, leading to a considerable improvement in accuracy, they found. A lot of recent studies have focused in the patella femoral osteoarthritis [17]. When compared to manual measurement, the automated JSW measurement provides more reliable results. An author [18] has manually measured the distance between the extremities of each femur and tibia in order to make a comparison. For this reason, the lateral JSW is less than the medial JSW, but with the automated technique the reverse is true. Researchers have employed a number of different methods to categories knee osteoarthritis, and these methods are compared in Table 4. These methods include support vector machines (SVMs), random forest classifiers (RFCs), and convolution neural networks (CNNs).

TABLE 4
ASSESSMENT OF CLASSIFICATION METHODS IN KOA: A SURVEY AND COMPARISON

Ref. No.	Dataset & Data Type	No.of Images Used	Algorithm	Result
[19]	OAI & X-ray	4130	DenseNet	Average Multi class accuracy is 71.08%
[20]	OAI, MOST & X-ray	OAI-19704 MOST-11743	Transfer Learning from Image Net	(i)Cohen's Kappa Co-eff is 0.82. (ii) FL-0.79 FM-0.84 (iii) TL-0.94 TM- 0.83

[21]	OAI & MRI	4384	CNN-DenseNet	(iv) JSN- 0.90 RF model: Sensitivity- 67.01%, Specificity- 71.79% DenseNet: Sensitivity- 76.99%, Specificity- 77.94%
[22]	Own dataset & MRI	1370	CNN- MRNet	AUC values: 0.937, ACL tears- 0.965, Menisci tears- 0.847.
[23]	OAI, MOST & X-ray	OAI- 4796, MOST- 3026	Deep Siamese CNN	Multiclass accuracy: 66.71%
[24]	Own & X-ray	140	HOG feature based template matching	Accuracy- 97.14%. F1 score- 98.40%. Cohen's Kappa-0.8507
[25]	OAI & X-ray	600	VGG19 & DenseNet	Accuracy 83.2% Sensitivity 80% Specificity 78%

III. Description of the Data

Researchers have worked using a wide variety of datasets, some of which have been made available to the public and others have been acquired independently. OAI, MOST, BLSA, and an OAI-derived data collection are only few of the popular publicly available data repositories. The majority of studies have made use of the OAI data set. Multiple methods of data gathering were used by certain researchers [15]. Few researchers, despite the need for such information, actually collect it because they find it interesting. The X-rays of the knee used here were from a publicly accessible database. The downloaded dataset was partitioned into a training set and a testing set with a 70:30 split. The information for this upcoming study will come from a private hospital. Test and training datasets are described in Table 5.

Table 5
Number of Images used for Training and Testing

Severity Stages	Number of Trained Data	Number of Tested Data
Normal	2286	639
Doubtful	1046	296
Mild	1516	447
Moderate	757	223
Severe	173	51
Total	5,778	1,656

IV. AlexNet Architecture

The majority of AlexNet applications are for object detection. ImageNet was made accessible to the public after it had won a competition for similar purposes. More than 15 million high-quality images are included in the ImageNet collection, which is divided into more than 22,000 categories.

Dropout is used in AlexNet to reduce the degree on a network that has been overworked. This is accomplished during the model's training phase by quickly turning off neurons at a predetermined rate. To be more precise, this is done so that the model can provide the expected outcomes. Because of this, the network becomes less sensitive on its local nodes and more capable of generalisation [26].

In contrast to prior neural networks, AlexNet uses the recurrent linear unit (ReLU) as its activation function. When compared to the more common sigmoid and "tanh" functions employed in other neural networks, this one is rather unique. In addition to improving the model's training speed, ReLU's non-saturated activation function also aids in reducing the issues of gradient disappearance and gradient explosion. This is because ReLU is an activation function that does not reach saturation. The immediate result of this is that training a more complicated network is an easy one [27, 29].

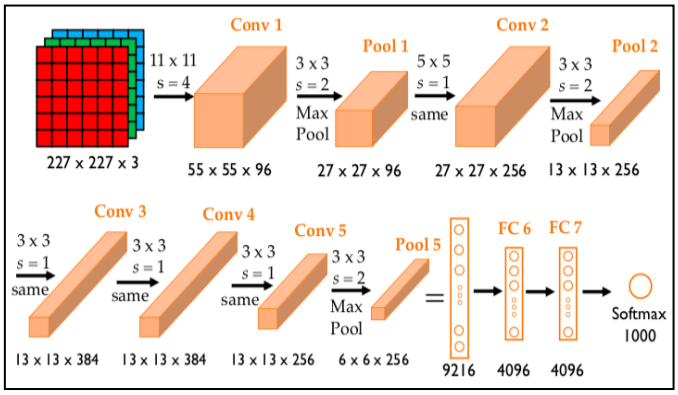

Fig. 3 Architecture of AlexNet model.

The eight layers that make up AlexNet are broken down into five convolution layers, three max-pooling layers, and three fully connected layers given in Table 6.

The fig. 3 above depicts the AlexNet Architecture. The input picture should have the following dimensions: 227x227x3, where '3' stands for the color image.

1) *1st Convolution Layer:* This layer takes a 227x227x3 pixel image as its input. With a stride of 4 pixels, the 96 filters in this convolution layer will each be 11x11 in size. There is no padding on this layer.

The dimensions of the final image are as follows:

$$\frac{n-f}{s}+1 * \frac{n-f}{s}+1 \qquad (1)$$

Here n indicated the input image size and f is the filter size and S is the stride. So after the 1st convolution layer the image size will be 55x55x96.

2) *1st Max Pooling layer*: In the pooling layer that follows the first convolution layer, we use a window size of 3x3 and a stride of 2 pixels to further decrease the image's overall size. This max pooling layer receives input from the previous layer's output (55x55x96). This layer's output image size is 27x27x96

3) *2nd Convolution Layer*: In this layer, 256 filters of size 5x5 with padding 2 are used to process the data produced by the first max pooling layer (27x27x96).

Here padding is used. So the formula is
With padding,

$$\frac{n+2p-f}{s}+1 \ * \ \frac{n+2p-f}{s}+1 \qquad (2)$$

Here p indicates the padding. This convolution layer will produce the image with the size of 27x27x256.

4) *2nd Max Pooling layer:* It has a window size of 3x3 and a stride of 2. It receives data from the layer below it. The final output of this layer will have a dimension of 13x13x256.

5) *3rd, 4th and 5th convolution layer*: Without a pooling layer in between, they are joined one to the other. The third and fourth convolution layers perform the same functions since they share the same characteristics, such as 384 filters with a 3x3 filter size and 1 bit of padding. The third and fourth convolution layers' images will be 13x13x384 in size. In the fifth convolution layer, the filter size is 3x3, although there are 256 filters and just one padding. This layer's output size is 13x13x256.

6) *3rd Max pooling layer:* This max pooling layer receives the output of the final convolution layer, and as a result, the final picture size is 6x6x256. The next step, after the convolution phase, is to do the object detection. Therefore, the fully connected layer must do the object detection.

7) *Fully connected Layers:* There are three fully connected layers. In the last layer, we use a soft-max activation function to calculate the output, which yields a distribution over a thousand labels representing different classes. First, second, and third layers are all fully connected, with 4096, 4096, and 1000 neurons, respectively. Each neuron will remember a unique class label. Now multiplying the dimensions of the two-dimensional picture (6x6x256) yields a single-dimensional image with 9216 pixels. The fully connected layer, which already has the 4096 neurons needed to analyze 9216 pixels, will receive the data.

All-digital X-ray images were too big, therefore we reduced their resolution to [227x227x3]. When the image size is too small, it will cause the image overlap and if the image size is too large then it will take more time to process then image to produce the training dataset [28].

TABLE 6
DETAILS OF ALEXNET PARAMETERS

Layers	Activation Shape	Activation Size	No of Parameters
Input Image	227x227x3	154587	0
Conv 1	55x55x96 (f=11, s=4, p=0)	290400	34944
Pool 1	27x27x96 (f=5, s=2)	69984	0
Conv 2	27x27x256 (f=5, s=1, p=2)	186684	614,656
Pool 2	13x13x256 (f=3, s=2)	43264	0
Conv 3	13x13x384 (f=3, s=1, p=2)	64896	885,120
Conv 4	13x13x384 (f=3, s=1, p=1)	64896	1,327,488
Conv 5	13x13x256 (f=3, s=1, p=1)	43264	884,992
Pool 5	6 x 6 x 256 (f=3, s=2)	9216	0
FC 3	4096 x 1	4096	37,748,737
FC 4	4096 x 1	4096	16,777,217
Softmax	1000 x 1	1000	4096001

A. *System frame work*

The majority of the effort will be spent on pre-processing and categorization. The dimensions of the images were changed to 227x227x3 to meet AlexNet's requirements. Fig. 4 displays the suggested approach for the categorization of KOA.

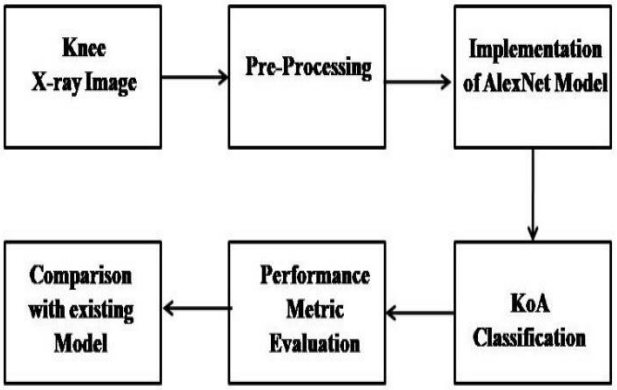

Fig. 4 Classification of KoA using AlexNet Model

V. RESULT AND DISCUSSION

Several different machine learning and Deep Learning approaches have been discussed above in relation to diagnosing and predicting KOA. Using segmentation techniques such as the canny edge detector, graph cut algorithm, principal component analysis, and generalised linear clustering, features were recovered from the space or the dimensionality of the space was decreased. SVMs, which are a kind of machine learning model, are used to direct the bulk of X-ray-based investigations and are responsible for guiding investigative judgments. The performance of Alexnet in identifying cases of knee osteoarthritis was examined with the help of a system written in Python and run on the colab

environment. As a first phase in the processing, the image is given a Gaussian Blur and then eroded shown in fig.5.

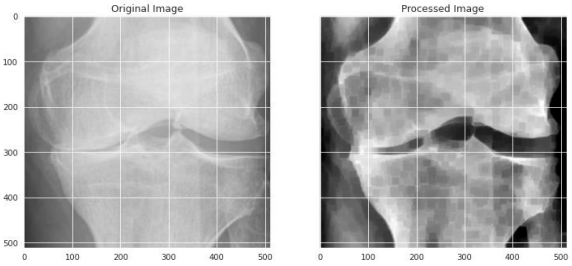

Fig. 5 Pre-processed image

The AlexNet model produced a classification accuracy of 98.62% shown in fig. 6. The same model is used for the OAI dataset but there are some challenges. On the basis of pre-processing, bilateral radiographs need to be divided in two parts and each part containing single knee. Without changing the image resolution, a appropriate data filtering technique to be used. Accurate Region of interest should be identified.

```
Epoch 95/100
181/181 [========]  - 24s 134ms/step  - loss:
0.0548 - accuracy:  0.9827
Epoch 96/100
181/181 [========]  - 24s 134ms/step  - loss:
0.0305 - accuracy:  0.9893
Epoch 97/100
181/181 [========]  - 25s 135ms/step  - loss:
0.0437 - accuracy:  0.9843
Epoch 98/100
181/181 [========]  - 24s 134ms/step  - loss:
0.0214 - accuracy:  0.9929
Epoch 99/100
181/181 [========]  - 24s 135ms/step  - loss:
0.0492 - accuracy:  0.9836
Epoch 100/100
181/181 [========]  - 25s 136ms/step  - loss:
0.0439 - accuracy:  0.9862
```

Fig. 6 Output of AlexNet for 100 epochs.

In order to evaluate AlexNet and see how well it stacks up against other models, we have tested it against Inception V3, DenseNet, MobileNet, and ResNet. The results of the various experiments conducted on the models are summarised in Table 7. According to the information in the table, it would seem that AlexNet is successful in identifying knee osteoarthritis.

TABLE 7
PERFORMANCE COMPARISON OF FIVE MODELS IN TERMS OF ACCURACY

Models	Accuracy (%)
Inception V3	83
DenseNet	84
MobileNet	71
ResNet	82
AlexNet	**98**

In this study, we classified pictures of knee osteoarthritis using KL-Graded using a CNN that was based on AlexNet. In studies, AlexNet has shown to perform better than previous approaches for identifying knee osteoarthritis (OA). The suggested AlexNet model is an appropriate model since it has a score of 98.62% in terms of its accuracy in classification. Because deep learning models function more effectively on larger datasets, increasing the size of the dataset might result in improved classification accuracy. If the techniques for feature extraction used in the pre-processing of the data are carefully considered, it may be possible to achieve higher levels of performance using deep learning.

REFERENCES

[1] Tiulpin A, Melekhov I, Saarakkala S. KNEEL: Knee anatomical landmark localization using hourglass networks. In *Proceedings of the IEEE/CVF International Conference on Computer Vision Workshops* 2019 (pp. 0-0).

[2] Tiulpin A, Thevenot J, Rahtu E, Saarakkala S. A novel method for automatic localization of joint area on knee plain radiographs. In *Scandinavian Conference on Image Analysis* 2017 Jun 12 (pp. 290-301). Springer, Cham.

[3] Mahmood N, Shah AS, Waqas A, Abubakar AD, Kamran SH, Zaidi SB. Image segmentation methods and edge detection: An application to knee joint articular cartilage edge detection. *Journal of Theoretical and Applied Information Technology*. 2015 Jan 10;71(1):87-96.

[4] Rosenberger C, Chabrier S, Laurent H, Emile B. Unsupervised and supervised image segmentation evaluation. In *Advances in image and video segmentation 2006* (pp. 365-393). IGI Global.

[5] Gornale SS, Patravali PU, Uppin AM, Hiremath PS. Study of segmentation techniques for assessment of osteoarthritis in knee X-ray images. *International Journal of Image, Graphics and Signal Processing (IJIGSP)*. 2019 Feb 1;11(2):48-57.

[6] Chai R. Otsu's image segmentation algorithm with memory-based fruit fly optimization algorithm. Complexity. 2021 Mar 26; 2021.

[7] Chan S, Dittakan K, El Salhi S. Osteoarthritis detection by applying quadtree analysis to human joint knee X-ray imagery. *International Journal of Computers and Applications*. 2022 Jun 3;44(6):571-8.

[8] Kim YJ, Lee SR, Choi JY, Kim KG. Using Convolutional Neural Network with Taguchi Parametric Optimization for Knee Segmentation from X-Ray Images. *BioMed Research International*. 2021 Aug 23;2021.

[9] Chadoulos CG, Tsaopoulos DE, Moustakidis S, Tsakiridis NL, Theocharis JB. A novel multi-atlas segmentation approach under the semi-supervised learning framework: Application to knee cartilage segmentation. *Computer Methods and Programs in Biomedicine*. 2022 Oct 28:107208.

[10] Anifah, L., Purnomo, M.H., Mengko, T.L.R. and Purnama, I.K.E. Osteoarthritis severity determination using self organizing map based Gabor kernel. In *IOP Conference Series: Materials Science and Engineering*. 2018 Feb.

[11] Bien, Nicholas et al. Deep-learning-assisted diagnosis for knee magnetic resonance imaging: Development and retrospective validation of MRNet. *PLoS medicine* vol. 15,11 e1002699. 27 Nov. 2018

[12] R. Dey, Z. Lu and Y. Hong. Diagnostic classification of lung nodules using 3D neural networks. IEEE 15th *International Symposium on Biomedical Imaging (ISBI 2018)*, 2018, pp. 774-778.

[13] Kokkotis, C., Ntakolia, C., Moustakidis, S. et al. Explainable machine learning for knee osteoarthritis diagnosis based on a novel

fuzzy feature selection methodology. *Phys Eng Sci Med* 45, 219–229 (2022).

[14] Gornale, Shivanand & U., Pooja & R., Ramesh. (2016). Detection of Osteoarthritis using Knee X-Ray Image Analyses: A Machine Vision based Approach. *International Journal of Computer Applications*. 145. 20-26. 10.5120/ijca2016910544.

[15] Kondal S, Kulkarni V, Gaikwad A, Kharat A, Pant A. Automatic grading of knee osteoarthritis on the Kellgren-Lawrence scale from radiographs using convolutional neural networks. In *Advances in Deep Learning, Artificial Intelligence and Robotics* 2022 (pp. 163-173). Springer, Cham.

[16] Dieppe, P., Cushnaghan, J., Young, P., & Kirwan, J. (1993). Prediction of the progression of joint space narrowing in osteoarthritis of the knee by bone scintigraphy. *Annals of the rheumatic diseases*, 52(8), 557–563.

[17] Bayramoglu N, Nieminen MT, Saarakkala S. Machine learning based texture analysis of patella from X-rays for detecting patellofemoral osteoarthritis. *International journal of medical informatics*. 2022 Jan 1;157:104627.

[18] Sugiyanto, S., Fatimah, F., Setia Budi, W., Suwondo, A., & Suyanto, H. (2021). Comparison of Joint Space Width Determinations in Grade I and II Knee Osteoarthritis Patients Using Manual and Automatic Measurements. *Journal of biomedical physics & engineering*, 11(5), 613–620.

[19] Y. Dalia, A. Bharath, V. Mayya and S. Sowmya Kamath, DeepOA: Clinical Decision Support System for Early Detection and Severity Grading of Knee Osteoarthritis. 2021 *5th International Conference on Computer, Communication and Signal Processing* (ICCCSP), 2021, pp. 250-255.

[20] Wang Y, Bi Z, Xie Y, Wu T, Zeng X, Chen S, Zhou D. Learning From Highly Confident Samples for Automatic Knee Osteoarthritis Severity Assessment: Data From the Osteoarthritis Initiative. *IEEE Journal of Biomedical and Health Informatics*. 2021 Aug 4;26(3):1239-50.

[21] Ebrahimkhani S, Dharmaratne A, Jaward MH, Wang Y, Cicuttini FM. Automated segmentation of knee articular cartilage: Joint deep and hand-crafted learning-based framework using diffeomorphic mapping. *Neurocomputing*. 2022 Jan 7;467:36-55.

[22] Oei EH, Van Zadelhoff TA, Eijgenraam SM, Klein S, Hirvasniemi J, Van Der Heijden RA. 3D MRI in Osteoarthritis. In *Seminars in Musculoskeletal Radiology* 2021 Jun (Vol. 25, No. 03, pp. 468-479). Thieme Medical Publishers, Inc.

[23] Tiulpin A, Thevenot J, Rahtu E, Lehenkari P, Saarakkala S. Automatic knee osteoarthritis diagnosis from plain radiographs: a deep learning-based approach. *Scientific reports*. 2018 Jan 29;8(1):1-0.

[24] Saleem M, Farid MS, Saleem S, Khan MH. X-ray image analysis for automated knee osteoarthritis detection. *Signal, Image and Video Processing*. 2020 Sep;14(6):1079-87.

[25] Guan B, Liu F, Mizaian AH, Demhri S, Neogi T, Guermazi A, Kijowski R. Deep learning approach to predict radiographic knee osteoarthritis progression. *Osteoarthritis and Cartilage*. 2019 Apr 1;27:S395-6.

[26] Hinton GE, Srivastava N, Krizhevsky A, Sutskever I, Salakhutdinov RR. Improving neural networks by preventing co-adaptation of feature detectors. *arXiv preprint arXiv:1207.0580*. 2012 Jul 3.

[27] Nair V, Hinton GE. Rectified linear units improve restricted boltzmann machines. InIcml 2010 Jan 1.

[28] Abu M, Amir A, Lean YH, Zahri NA, Azemi SA. The performance analysis of transfer learning for steel defect detection by using deep learning. *InJournal of Physics: Conference Series* 2021 Feb 1 (Vol. 1755, No. 1, p. 012041). IOP Publishing.

[29] Rakesh G, Rajamanickam V. A Novel Deep Learning Algorithm for Optical Disc Segmentation for Glaucoma Diagnosis. *Traitement du Signal*. 2022 Feb 1;39(1).